Pergamon

Int. J. Solids Structures Vol. 31, No. 6, pp. 807–822, 1994
Elsevier Science Ltd
Printed in Great Britain
0020–7683/94 $6.00 + .00

AN EXPERIMENTAL AND THEORETICAL INVESTIGATION OF THE RESPONSE OF BS11 STEEL TO CYCLIC LOADING

X. PENG
Department of Engineering Mechanics, Chongqing University, Chongqing 630044, People's Republic of China

and

A. R. S. PONTER
Department of Engineering, University of Leicester, Leicester LE1 7RH, U.K.

(*Received* 26 *May* 1993; *in revised form* 10 *September* 1993)

Abstract—This paper contains a detailed experimental investigation of the cyclic properties of a standard high-carbon pearlitic rail steel (BS11) subjected to complex uniaxial cyclic loading. The experiments were designed to be either load- or strain-controlled. It is found that the material response strongly depends on the mean value of stress or plastic strain as well as its amplitude. In a strain-controlled process, the mean stress does not reduce to zero but to a value corresponding to the plastic mean strain assuming the amplitude is kept constant. The specimen ratchets in the direction of mean stress but the cyclic ratcheting rate greatly reduces during the cyclic process and ends at a constant value. There is no sign that the ratcheting would stop, which is a new observed feature different from Bower's observation. The constitutive description proposed by the authors is found to give a good correlation to the experimental observation.

1. INTRODUCTION

The plastic flow of railway track under repeated loading has attracted extensive attention because increasing evidence reveals that both the sliding wear and the initiation of contact fatigue cracks may be attributed to the near surface plastic deformation (Bower, 1989). In repeated rolling and sliding contact railway track almost invariably suffers from some degree of plastic deformation which is driven by the high normal and tangential stress acting between the wheel and rail track. Plastic strain is accumulated by each successive pass of the wheel to an intolerant amount over thousands of cycles. It is therefore important to understand the material property of rail steel subjected to complex cyclic loading history. For this purpose, Bower (1987, 1989) made an experimental study of rail steel BS11. He found that this material possesses a remarkable property called locking-in inter-phase residual stress capability (Bower, 1987). Specifically, the capability to store the energy in the internal structures when plastic deformation is not uniform in different phases, and this part of the energy can be released when the deformation returns to a uniform state in the following cyclic process. It was found that in a tension/compression test a rail steel specimen ratchets in the direction of mean load, but the ratcheting rate gradually decreases and finally vanishes when the cyclic number is sufficiently large. Further, if the mean load is removed the specimen will ratchet in the opposite direction although there exists no mean load. By the end of the test the specimen virtually returned to its original length. If a specimen is at first subjected to an unsymmetrical cycle of torque the specimen duly accumulates a twist in the direction of mean torque. Then letting the same specimen suffer a fully reserved tension/compression, the specimen will unwind gradually. During each cycle the accumulative twist of the specimen gradually decreases despite the fact that no torque is applied during the test. By the end of the test the specimen has virtually lost the twist accumulated during the torsion test. This kind of phenomenon is not observed to occur in OFHC specimens (Bower, 1989; Bower and Johnson, 1990). Although this work is of considerable interest, the obtained result is insufficient for a systematic understanding of the response of this kind of material even in uniaxial cases.

A detailed experimental investigation of the properties of rail steel BS11 subjected to complex uniaxial cyclic loading has been made in this work. All of the tests were conducted on a computer-controlled servo-hydraulic testing machine. The load was measured with a load cell and the strain by an extensometer attached to the uniform section of the specimens. The experiment was either load- or strain-controlled. The effect of both the mean value and the amplitude of stress or strain on the material response was investigated. It was observed that in a strain-controlled process, the mean stress would not reduce to zero but to a value corresponding to the given plastic mean strain assuming the amplitude is kept constant. In a stress-controlled process, the specimen ratcheted in the direction of mean stress but the ratcheting rate greatly reduced during the cyclic process and tended to a constant value. It should be mentioned that there was no sign that the ratcheting would stop even if a specimen had suffered thousands of cycles until fracture. The model recently developed by Peng and Ponter (1993), which involves the influence of the history and the present state of stress and plastic strain on constitutive response, is used to analyse the experimental results and gives a satisfactory correlation with the observed phenomenon.

2. EXPERIMENTAL ARRANGEMENT AND THE MAIN RESULTS

The specimens were cut from the head of a railway track in a normal state. The longitudinal direction of the specimen is parallel to the longitudinal direction of the railway track. The composition of the specimen is listed in Table 1. A metallograph of the virgin material along with the longitudinal section of the specimen is shown in Fig. 1(a), it is seen from which that the material mainly consists of pearlite and ferrite.

Figure 2 shows the geometry of the specimen in which a hole of diameter D_i along the axis of the specimen is drilled for two purposes: (1) to prevent the specimen from buckling during compression and (2) to reduce the maximum load to the range of the testing machine. An Instron uniaxial extensometer with 25 mm gauge length was used to measure axial strain. This extensometer was attached to the surface of the uniform part of the specimen and measured the average axial strain of this part directly. The load (stress) was measured by the load cell. The nominal stress is expressed by σ. By using the assumption that the material is plastically incompressible and neglecting the elastic volumetric deformation, the true stress can be approximately calculated by

$$\sigma_t = (1+\varepsilon)\sigma \tag{1}$$

in which ε is nominal axial strain, which satisfies

$$A = \frac{l_0}{l} A_0 = \frac{A_0}{1+\varepsilon}, \tag{2}$$

where A and A_0 are the present and original cross-section areas. In this paper the nominal stress and strain were adopted unless otherwise stated.

All the tests were conducted on a microcomputer-controlled servohydraulic testing machine. The controlled strain (or load) and the response load (or strain) are directly plotted to an X–Y recorder and recorded by the computer.

Table 1. Composition of used BS11 (normal grade)

C	Mn	P	Cr	Al
0.56%	1.13%	0.029%	0.04%	<0.01%
S	Si	Ni	Mo	Ti
0.029%	0.27%	0.02%	<0.01%	0.01%

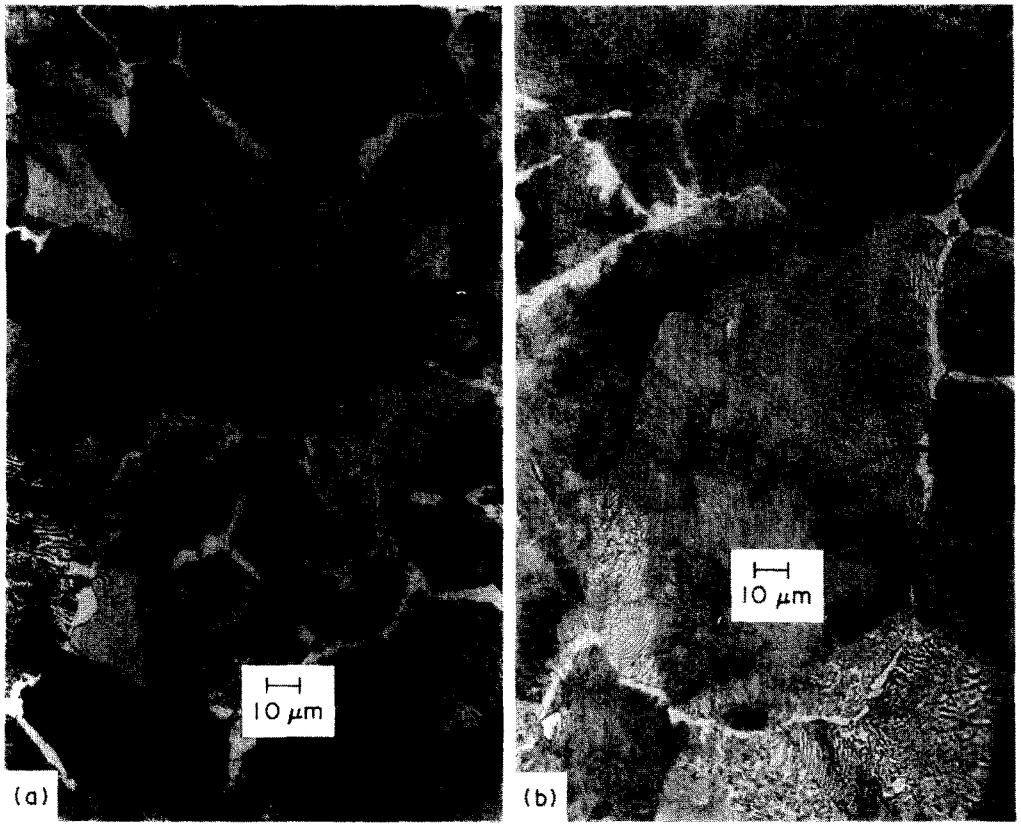

Fig. 1. Metallographs of the longitudinal section. (a) Before text and (b) after text.

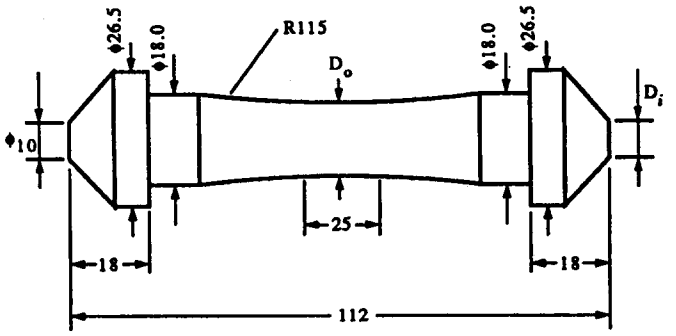

Fig. 2. The geometry of the specimen.

The effect of the mean value and amplitude of strain or stress on the constitutive response respectively was experimentally investigated, thus the following tests were arranged:

1. Strain-controlled monotonic loading.
2. Strain-controlled cyclic loading with various mean strains and a fixed strain amplitude.
3. Strain-controlled cyclic loading with a fixed mean strain and various strain amplitudes.
4. Stress-controlled cyclic loading with various mean stresses and a fixed stress amplitude.
5. Stress-controlled cyclic loading with a fixed mean stress and various stress amplitudes.

The detailed arrangements of these tests are given in Tables 2 and 3. It should be noted that several segments with differing governing parameters were performed on each specimen

Table 2. Summary of strain-controlled tests

Test No.	Segment	Diameter (mm) D_0, D_i	ε_m (%)	ε_a (%)	Cyclic number
1	1	14.34, 9.54	0	0.4	200
	2		0	0.6	20
	3		0	0.8	20
	4		0	1.0	20
	5		0	1.2	20
	6		0	1.0	20
	7		0	0.8	20
	8		0	0.6	20
	9		0	0.4	20
2	1	14.40, 9.54	0.4	0.4	100
	2		0.0	0.4	100
	3		0.4	0.6	100
	4		0.0	0.6	100
	5		0.4	0.8	100
	6		0.0	0.8	100
3	1	14.40, 9.54	0.2	0.6	100
	2		0.0	0.6	100
	3		0.4	0.6	100
	4		0.0	0.6	100
	5		0.6	0.6	100
	6		0.0	0.6	100
	7		0.6	0.6	100
	8		0.0	0.6	100
	9		0.4	0.6	100
	10		0.0	0.6	100
	11		0.2	0.6	100
4		14.32, 9.70	0.0	0.6	2890
5		14.20, 10.0	0.3	0.6	2280

Table 3. Summary of stress-controlled tests

Test No.	Segment	Diameter (mm) D_0, D_i	σ_m (MPa)	σ_a (MPa)	Cyclic number
6	1	14.40, 9.54	52.5	475	200
7	1	14.00, 9.54	25.0	450	600
	2		0.0	450	600
	3	14.30, 9.54	51.0	450	600
	4		0.0	450	600
	5	14.45, 9.54	38.0	450	600
	6		0.0	450	600
	7		−38.0	450	600
	8		0.0	450	600
8	1	14.34, 9.54	30.0	380	600
	2		0.0	380	400
	3		30.0	420	600
	4		0.0	420	400
	5		30.0	460	600
	6		0.0	460	400
9	1	14.10, 9.68	25.0	450	3100

due to the experimental fact that the previous deformation history only slightly affects the successive cyclic constitutive response for the adopted material. However, some additional segments were also included to make the material return to its original state as much as possible. All of the tests were conducted at room temperature. To make the deformation process smooth the sine-shaped wave form was chosen for cyclic loading and the frequency was chosen as 0.15 Hz which might exclude the rate effect from the experimental results.

Table 2 contains five strain-controlled tests, with which the properties of the material under strain-controlled cycling are investigated. In test 1 the specimen was subjected to symmetrically cyclic straining, in which nine segments with different strain amplitude were included. With the results of this test the cyclic hardening behaviour and the memory of the cyclic strain history may be investigated. Test 2 involves six segments with different strain amplitude $\varepsilon_a = 0.4\%$, 0.6% and 0.8%, and a fixed mean strain $\varepsilon_m = 0.4\%$. This test was designed for the purpose of investigating the effect of strain amplitudes on the stress response when a mean strain exists. Each segment contained 100 cycles which would probably ensure that the steady-state of stress is reached. Between the two segments with different strain amplitudes, a segment with zero mean strain is arranged, in which the variation of the mean stress formed in the previous cyclic process may be observed, and the effect of the previous mean strain history may be erased. In test 3 the relation between mean strain and the stress response under a fixed medium strain amplitude $\varepsilon_a = 0.6\%$ was researched. Eleven segments were included, which covers $\varepsilon_m = 0.2\%$, 0.4% and 0.6%. Tests 4 and 5 are designed to investigate the variation of the mean stress during the whole strain-controlled cyclic process with or without the existence of mean strain.

There are four stress-controlled tests in Table 3. Test 6 as well as test 1 was used for the determination of the material constants. Test 7 included eight segments with fixed stress amplitude $\sigma_a = 450$ MPa and mean stress $\sigma_m = 25$, 51, 38, and -38 MPa, in which the effect of mean stress on the variation of accumulated strain was to be observed. Each segment contains 600 cycles for the consideration that a steady cyclic ratcheting state is reached. Test 8 included six segments with fixed mean stress $\sigma_m = 30$ MPa and stress amplitude $\sigma_a = 380$, 420 and 460 MPa, from which the variation of the accumulated strain against the variation of stress amplitude was observed. In tests 7 and 8, some segments with $\sigma_m = 0$ were arranged for the purpose of erasing the memory of the previous mean stress history and to observe the variation of previous accumulated strain in the following cyclic process with the mean stress removed. Test 9 was a critical test that was used to observe whether the cyclic ratcheting will stop or not even after thousands of cycles until fracture under the condition of $\sigma_a = 450$ MPa and $\sigma_m = 25$ MPa.

The solid curve in Fig. 3 is the σ–ε relation of BS11 subjected to monotonic tension and with strain rate $\dot{\varepsilon} = 10^{-3}$/s. It was obtained from the test that the elastic modulus

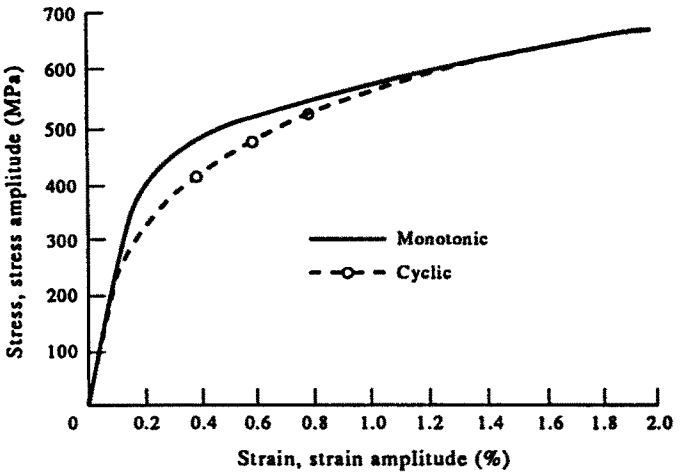

Fig. 3. Relations between uniaxial stress and strain.

$E = 203.5$ GPa. There exists strong strain hardening as plastic deformation develops. No distinct yield point is observed, and the transition from elastic to plastic hardening state is gradual and smooth. The experimental data was recorded until $\varepsilon = 2\%$ due to the range of the extensometer, which, fortunately, covered the range required in this experimental programme.

Figure 4(a) shows the experimental hysteresis loops corresponding to the last cycles of segments 1–5 in test 1. The experimental saturated hysteresis loops corresponding to the segments 5–9 in the same test do not remarkably differ from that in Fig. 4(a), i.e. the cyclically saturated state of this material does not "remember" the previous cyclic hardening or softening history. The relation between the stress and strain amplitudes at saturated state (cyclic σ_a–ε_a curve) is also plotted in Fig. 3, shown with a dashed curve. Compared with the monotonic σ–ε curve, some degree of cyclic softening is observed. It is seen from the experimental result that the absolute value of the negative peak stress is larger than that of the positive one even if they are plotted in the real stress and strain space although there exists no mean strain. In Fig. 4(b) the solid line shows the experimental relation between nominal mean stress σ_m and plastic strain amplitude ε_a^p, where it is found that this relation is almost linearly proportional and can be approximately expressed by

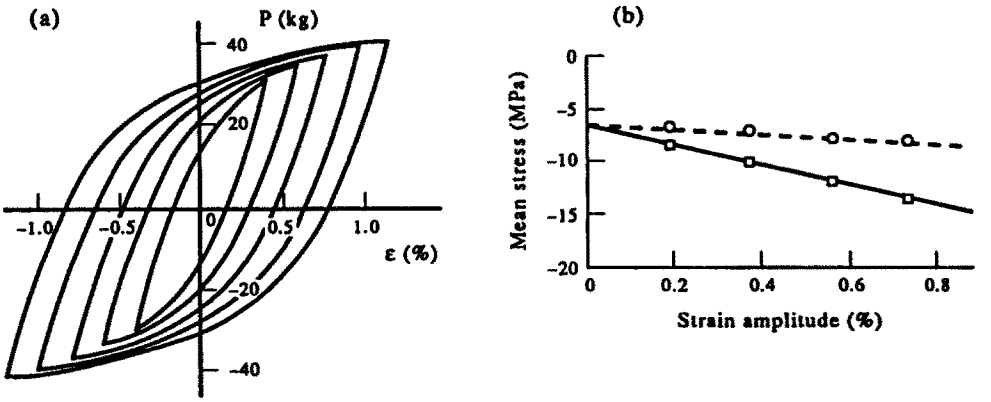

Fig. 4. Stress response under symmetrically strain-controlled test. (a) Hysteresis loops and (b) the variation of σ_m^0 vs ε_a.

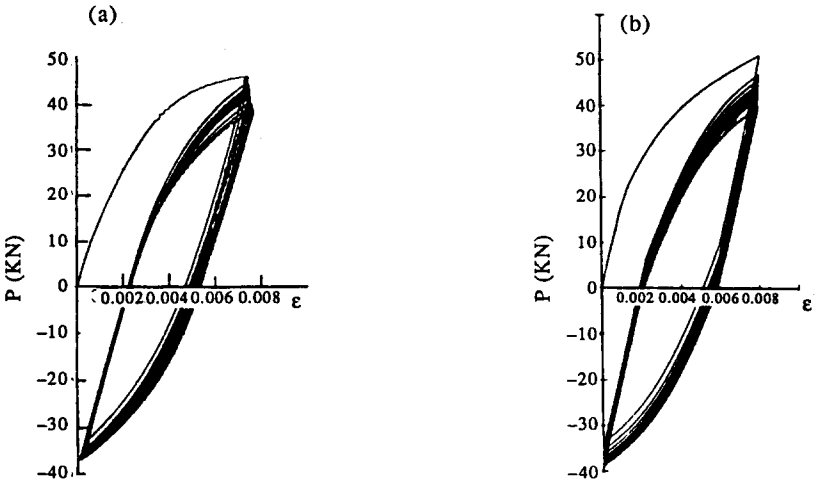

Fig. 5. Cyclic load response corresponding to $\varepsilon_a = \varepsilon_m = 0.4\%$. (a) Experimental and (b) theoretical.

$$\sigma_m^0 = -6.5 - 937.5\varepsilon_a^p \text{ (MPa)}. \tag{3}$$

The dashed line in Fig. 4 shows the experimental relation between mean value of true stress σ_{tm} calculated from eqn (1) and logarithmic plastic strain amplitude ε_{ta}^p, which is also nearly linear and can approximately be expressed as

$$\sigma_{tn}^0 = -6.5 - 250\varepsilon_{ta}^p \text{ (MPa)} \tag{4}$$

This phenomenon may be attributed to defects such as micro-cracks in the material which reduce the effective area in tension.

The experimental load against strain corresponding to the segment 1 in test 2 is shown in Fig. 5(a), in which it is seen that the mean load decreases during cyclic process. It is also found that the stress amplitude decreases, which implies that cyclic softening occurs when the strain amplitude is fixed (Fig. 6). Figure 7(a) shows the variation of mean load P_m against cyclic number N. It is seen that as the cyclic number increases the absolute value of mean load decreases and approaches a value corresponding to the given strain amplitude. Figure 7(b) shows the experimental relation between P_m and the strain amplitude at the last cycle of each segment in test 2, where P_m decreases when ε_a increases. It is found from this test that the saturated stress amplitudes of the segments 2, 4 and 6 are almost identical to those of segments 1, 2 and 3, which again indicates that stress amplitude is only slightly

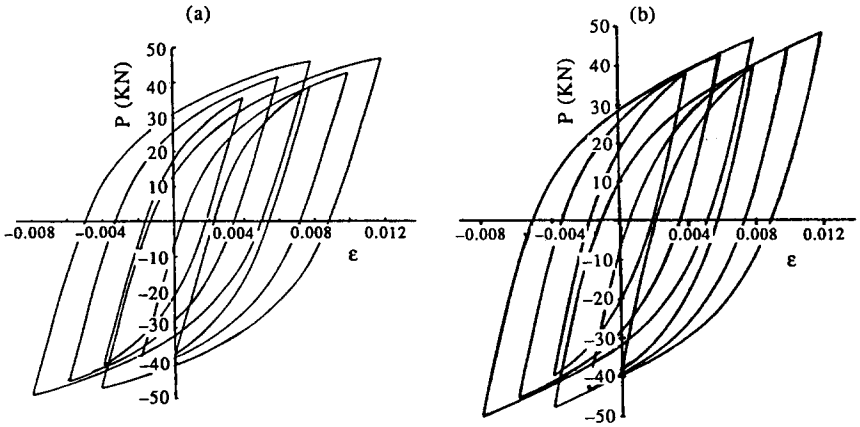

Fig. 6. Saturated loops under varying strain cycles. (a) Experimental and (b) theoretical.

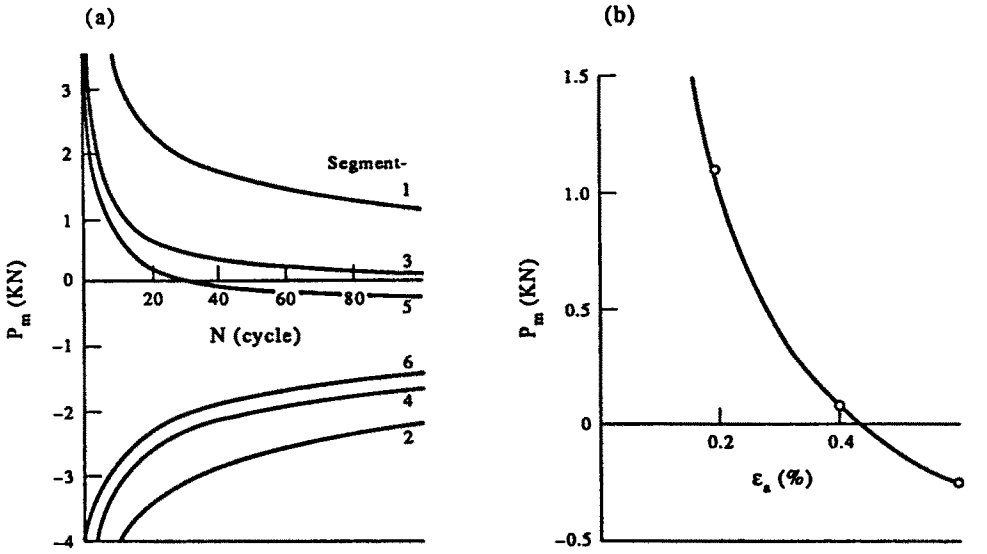

Fig. 7. Variations of P_m. (a) Variations of P_m vs cyclic number N and (b) variation of P_m vs ε_a (segments 1–6).

affected by deformation history, while stress amplitude slightly decreases when a mean strain exists.

The variations of P_m vs N in test 3 are shown in Fig. 8(a). For any individual curve the variation is similar to that in Fig. 7(a). Figure 8(b) gives the experimental relation between P_m and ε_m under a fixed strain amplitude $\varepsilon_a = 0.6\%$ at the last cycle of each segment in test 3, where it is observed that the mean load increases as the mean strain increases. It is also noticed that a negative mean load exists even if no negative mean strain is exerted on the specimen. This phenomenon is in agreement both qualitatively and quantitatively with that observed in test 1 (see Fig. 4b). The dashed circle in Fig. 8(b) is just the result of test 1 when $\varepsilon_a = 0.6\%$, which may be regarded as the asymptotic point of segments 2, 4, 6, 8 and 10 when the cyclic number is sufficiently large. It is also found that the relation between P_m (or σ_m) and ε_m is approximately linear if ε_a stays constant (see Fig. 8b).

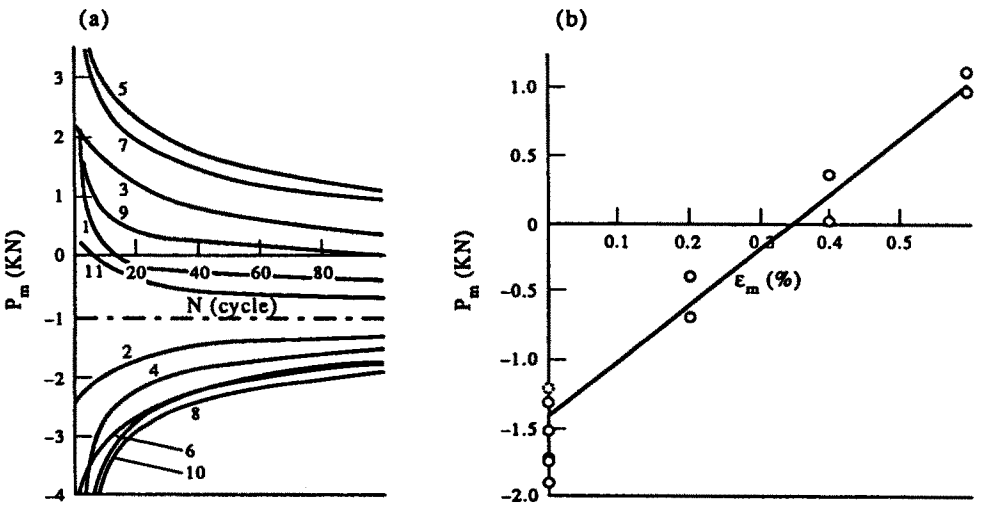

Fig. 8. Variations of P_m. (a) Variations of P_m vs cyclic number N and (b) variation of P_m vs ε_m.

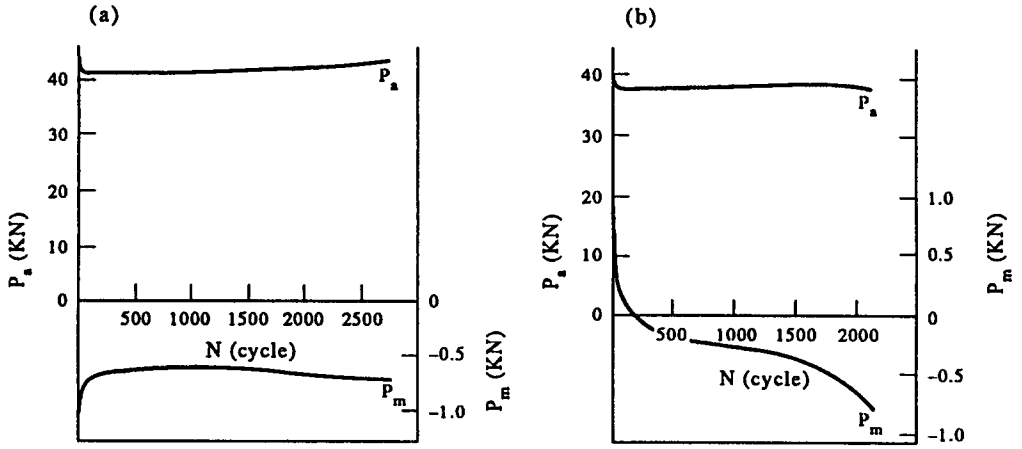

Fig. 9. Variations of P_a and P_m against N in strain-controlled cyclic processes. (a) $\varepsilon_a = 0.6\%$, $\varepsilon_m = 0$ and (b) $\varepsilon_a = 0.6\%$, $\varepsilon_m = 0.3\%$.

In test 4 the specimen was cycled under symmetrically strain-controlled conditions with $\varepsilon_a = 0.6\%$ to about 2890 cycles when fracture occurred. The variations of P_a and P_m against N are shown in Fig. 9(a), in which it is seen that P_a decreases in the first few cycles and then slightly increases as the cyclic number N increases, and this tendency is maintained until fracture occurs. The variation of P_m is quite similar to that of P_a. It should be mentioned that there is no sign that P_m would relax to zero, which means that under strain-controlled test conditions the stress response of this material is asymmetric in tensile and compressive processes.

In test 5, the specimen was subjected to cyclic strain with $\varepsilon_a = 0.6\%$ and $\varepsilon_m = 0.3\%$. The test stopped when a 2 mm long crack at the outer surface of the specimen was observed. The relations between P_a–N and P_m–N are plotted in Fig. 9(b). It is observed that the variation of P_a is similar to that in test 4 before cycle 1500. P_m varies from the value corresponding to the given ε_m to a negative value although the given ε_m is positive. After cycle 1500, P_a decreases slightly and the absolute value of P_m increases. Both the variations may be attributed to the damage of the material.

Following test 2 the same specimen was subjected to a stress-controlled cyclic process with the governing parameters listed in Table 2 (test 6). Figure 10(a) shows the experimental relation between the load P and the strain ε in this cyclic process. Figures 10(c) and (d) show the variations of the mean strain ε_m and the ratcheting rate $\mathrm{d}\varepsilon_m/\mathrm{d}N$ against cyclic number N, respectively. It is seen that cyclic ratcheting develops as cyclic number increases, the ratcheting rate decreases sharply at the beginning of the cyclic process and gradually tends to a constant.

The variation of ε_m and $\mathrm{d}\varepsilon_m/\mathrm{d}N$ against N corresponding to segments 1 and 5 of test 7 are shown in Fig. 11(a) and (b). It is seen that ε_m develops in the direction of σ_m and the rate $\mathrm{d}\varepsilon_m/\mathrm{d}N$ gradually decreases and tends to an asymptotic value corresponding to the given σ_m. It is also found that the ratcheting rate increases when σ_m increases (see Fig. 11c), but the absolute value of the ratcheting rate corresponding to positive σ_m is greater than that corresponding to a negative one, even though their absolute values of σ_m are the same. This again indicates that the constitutive response is asymmetric.

Figure 12 shows the influence of σ_a on $\mathrm{d}\varepsilon_m/\mathrm{d}N$ when σ_m is maintained constant (see segments 1, 3 and 5 in test 8), in which it is seen that $\mathrm{d}\varepsilon_m/\mathrm{d}N$ increases if σ_a increases. It is also found in this test that ε_a is only slightly affected by the exerted mean stress. It is seen from the comparison between segments 1 and 2, 3, and 4, or 5 and 6 that ε_a slightly increases if σ_m exists.

It should be mentioned that in the work by Bower (1987) and Bower and Johnson (1990) it was found that the ratcheting rate should stop for this kind of material when the

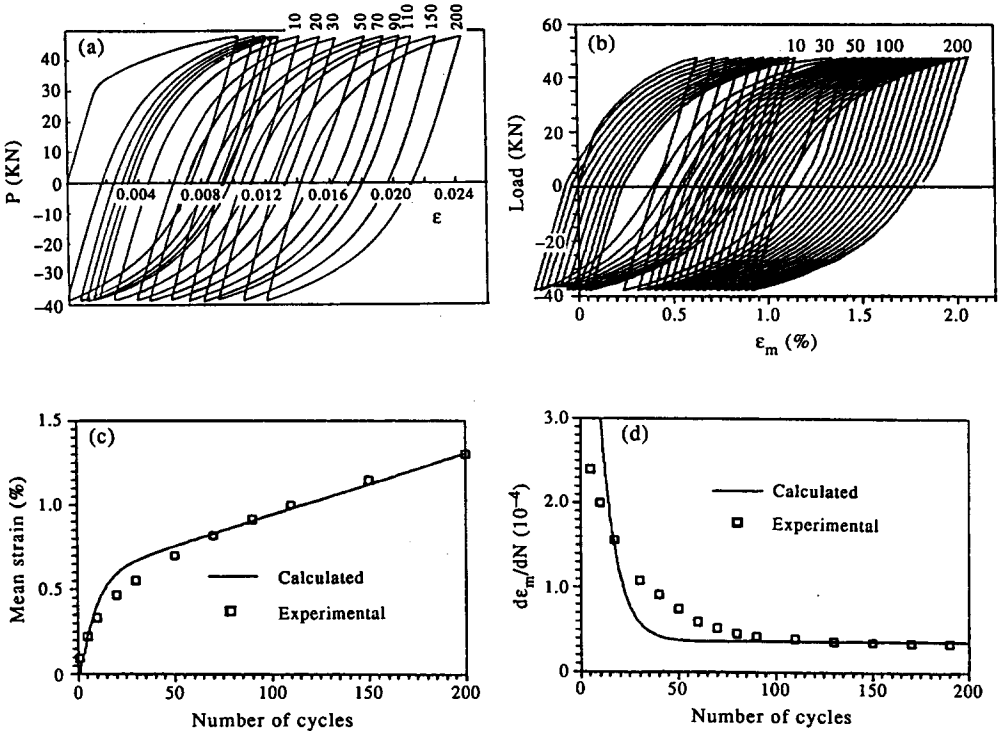

Fig. 10. Results of test 6. (a) Experimental relation between P and ε, (b) theoretical relation between P and ε, (c) variation of ε_m vs N and (d) variation of $d\varepsilon_m/dN$ vs N.

cyclic number is sufficiently large. In test 9 the specimen was subjected to about 3400 cycles with $\sigma_a = 450$ MPa and $\sigma_m = 25$ MPa when the ratcheting rate began to increase. Figure 13(a) shows the relation between P and ε in the cyclic process and Fig. 13(b) shows the variations of ε_m and $d\varepsilon_m/dN$ versus N. The ratcheting rate became steady at about $N = 1500$ and then remained constant until 3100 cycles when $d\varepsilon_m/dN$ began to increase (fracture occurred at about $N = 3400$). Figure 1(b) shows a metallograph of the longitudinal section of this specimen after fracture, in which a distinct crack going across the grains and perpendicular to the loading direction can be seen. Some cracks along the grain boundaries can also be detected. This is a typical characteristic of fatigue which indicates that the material has suffered a severe fatigue damage in the cyclic process. There is no direct evidence of continuum damage as a failure mechanism although the non-symmetry of the hysteresis loop could be attributed to micro-cracking. During the cyclic process there was no sign that the ratcheting would cease. The difference between the conclusion of Bower (1987) and Bower and Johnson (1990) and the present experimental result cannot be simply attributed to the difference between true and nominal stresses as the accumulative strain in the whole process is no more than 1.5%. The mechanism of the phenomenon appeared in this test is, in nature, similar to that in tests 4 and 5 where the mean stress did not relax to zero even after thousands of strain cycles.

3. CONSTITUTIVE EQUATION

It is seen from the experimental observation that the main features are similar to that reported by Bower for the two-phase materials with locking-in inter-phase residual stress capability. When macroscopic plastic deformation occurs, some phases suffer pure plastic deformation while other phases are still in an elastic or elastic–plastic state, and the corresponding elastic energy offers the possibility that the material will be restored to some extent in successive cyclic deformation.

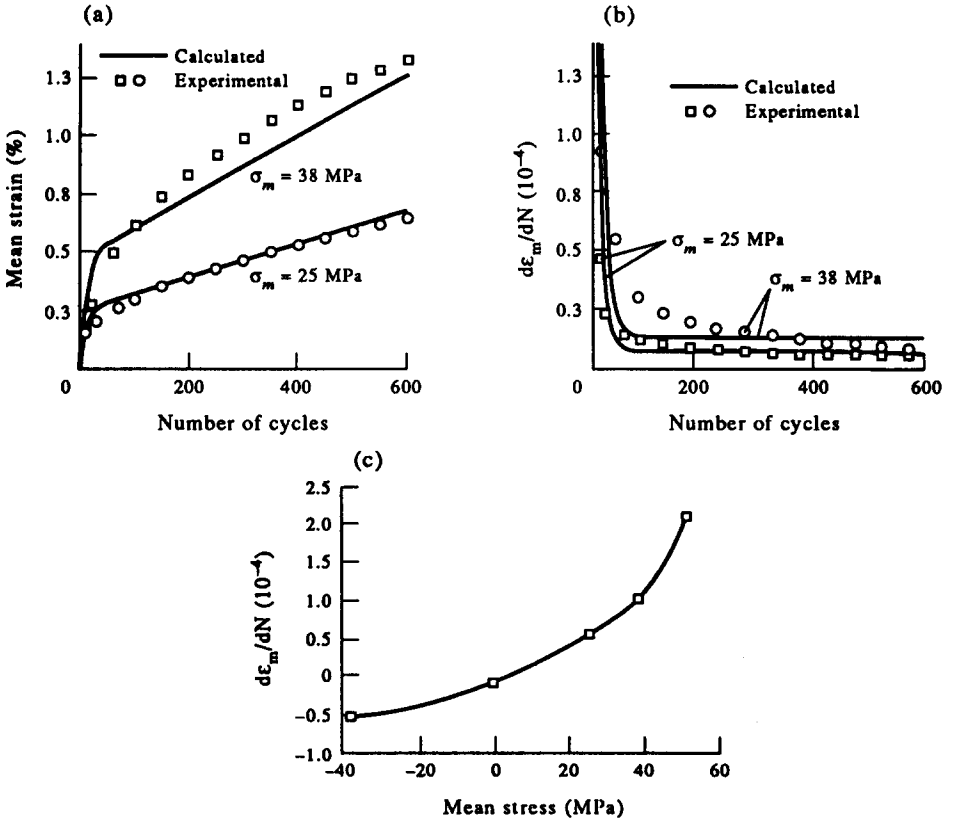

Fig. 11. Results of test 7. (a) Variation of ε_m vs N (segments 1 and 5), (b) variation of $d\varepsilon_m/dN$ vs N (segments 1 and 5) and (c) relation between $d\varepsilon_m/dN$ and σ_m.

Based on the assumption of isotropy and plastic incompressibility, and under the condition of isothermal and small deformation, a constitutive equation for this kind of material was proposed (Peng and Ponter, 1993) as follows:

$$s_{ij} = s_y^0 f(z) \frac{de_{ij}^p}{d\zeta} + \sum_{r=1}^{2} Q_{ij}^{(r)}, \tag{5}$$

where s_{ij} denotes deviatoric stress, e_{ij}^p deviatoric plastic strain, s_y^0 initial deviatoric yield stress, and $f(z)$ is a hardening function which is closely related to the internal structures of the material and is defined by

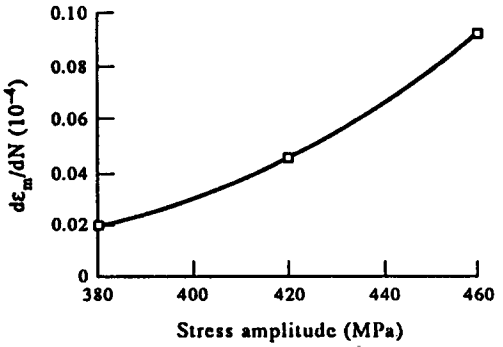

Fig. 12. Variation of $d\varepsilon_m/dN$ vs σ_a (test 8).

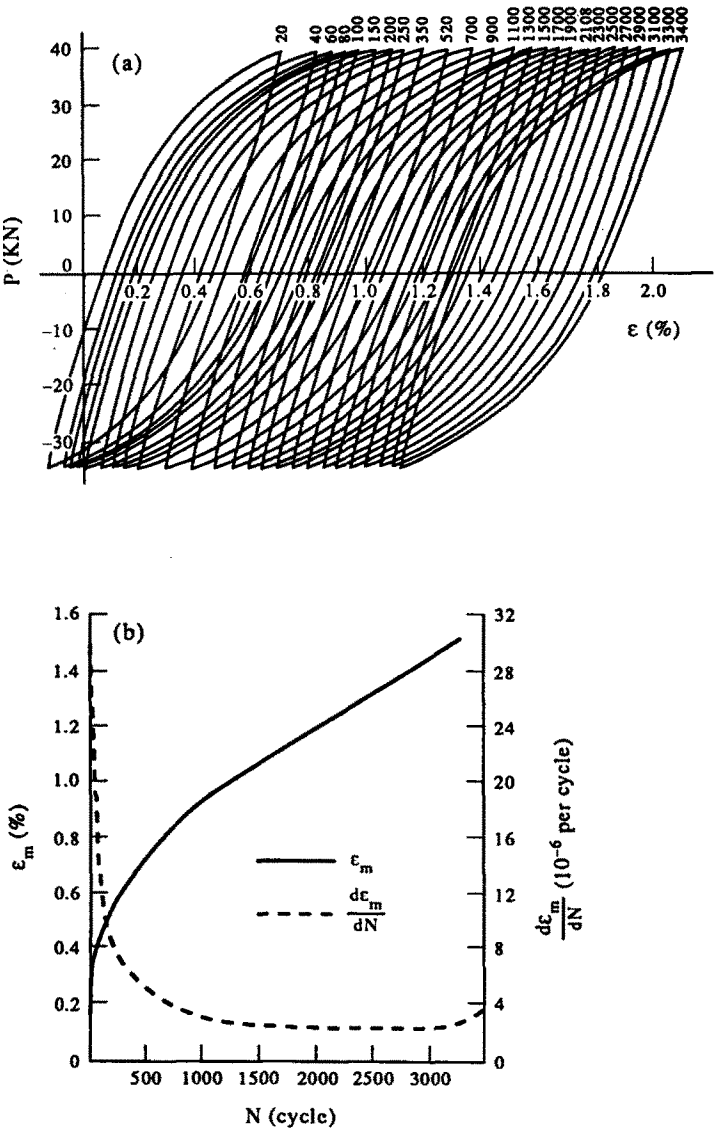

Fig. 13. Result of test 9. (a) P–ε curve in fatigue process and (b) variations of ε_m and $d\varepsilon_m/dN$ vs N.

$$\frac{df(z)}{dz} = \beta(c - f(z)) \quad \text{with } f(0) = 1 \tag{6}$$

in which z is the intrinsic time that can be expressed as (Wu and Yang, 1983)

$$dz = \frac{d\zeta}{f(z)}, \quad d\zeta = \|de_{ij}^p\|. \tag{7}$$

In a cyclic deformation process the material response depends strongly on cyclic hardening (or softening) which is closely related to the plastic strain amplitude (Fan and Peng, 1991), thus the parameter c in eqn (6) should be related to plastic strain amplitude characterized by the parameter ρ (Fan and Peng, 1991) and takes the following form in this work

$$c = \gamma_1 + \gamma_2(\gamma_3 + \rho)^{\gamma_4}. \tag{8}$$

$\Sigma Q_{ij}^{(r)}$ in eqn (5) is the back stress or the position of the centre of the yield surface, the component $Q_{ij}^{(r)}$ can be expressed as (Peng and Ponter, 1993)

$$Q_{ij}^{(r)} = \int_0^z \mathrm{e}^{-\alpha_r(z-z')}\left[E_r \frac{\mathrm{d}e_{ij}^p}{\mathrm{d}z'} + \beta_r\gamma_r\Omega_{ij}^{(r)}(z') + \beta_r E_r(e_{ij}^p(z') - \gamma_r\eta_{ij}^{(r)}(z'))\right]\mathrm{d}z' \tag{9}$$

in which

$$\Omega_{ij}^{(r)} = \int_0^z \mathrm{e}^{-\gamma_r(z-z')}\, Q_{ij}^{(r)}(z')\,\mathrm{d}z'$$

$$\eta_{ij}^{(r)} = \int_0^z \mathrm{e}^{-\gamma_r(z-z')}\, e_{ij}^p(z')\,\mathrm{d}z'. \tag{10}$$

The incremental form of $Q_{ij}^{(r)}$ can be expressed as

$$\Delta Q_{ij}^{(r)} = A_r \Delta e_{ij}^p + B_{ij}^{(r)}\Delta z, \tag{11}$$

where

$$\begin{aligned} A_r &= \kappa_r E_r \\ B_{ij}^{(r)} &= \kappa_r[\beta_r\gamma_r\Omega_{ij}^{(r)}(z_n) + \beta_r E_r(e_{ij}^p(z_n) - \gamma_r\eta_{ij}^{(r)}(z_n)) - \alpha_r Q_{ij}^{(r)}(z_n)] \\ \kappa_r &= \frac{1-\mathrm{e}^{-\alpha_r\Delta z}}{\alpha_r\Delta z}. \end{aligned} \tag{12}$$

The incremental form of the constitutive equation can be expressed in the form similar to that derived by Watanabe and Atluri (1984)

$$\Delta s_{ij} = 2\mu\left[\Delta e_{ij} - \frac{(s_{ij}-r_{ij})(s_{kl}-r_{kl})}{C(s_y^0)^2[f(z)]^2}\Gamma\Delta e_{kl}\right], \tag{13}$$

where μ is the elastic shear modulus and

$$\begin{aligned} r_{ij} &= \sum_{r=1}^{2} Q_{ij}^{(r)} \\ C &= 1 + \sum_{r=1}^{2} A_r + \frac{(s_{ij}-r_{ij})h_{ij}}{s_y^0 f(z)^2} + \frac{s_y^0 f(z)}{2\mu}\frac{\mathrm{d}f(z)}{\mathrm{d}z} \\ h_{ij} &= \sum_{r=1}^{2} \frac{B_{ij}^{(r)}}{2\mu} \\ \Gamma &= \begin{cases} 1, & \text{if } \|s_{ij}-r_{ij}\| = s_y^0 f(z) \text{ and } (s_{ij}-r_{ij})\,\mathrm{d}e_{ij} > 0 \\ 0, & \text{otherwise.} \end{cases} \end{aligned} \tag{14}$$

In the uniaxial tension and compression, $e_{22}^p = e_{33}^p = -0.5e_{11}^p$, $s_{22} = s_{33} = -0.5s_{11}$, $\sigma = 1.5s_{11}$; $\varepsilon = \sigma/E + e_{11}^p$, where E denotes Young's modulus. Using eqn (13) we have

$$\Delta s_{11} = 2\mu[1 - \tfrac{3}{2}a(s_{11}-r_{11})^2\Gamma]\Delta e_{11} \tag{15}$$

or

Table 4. Material constants of BS11

μ, E	80.12, 203.5 GPa
s_y^0	180 MPa
$E_{1,2}$	112, 18.6 GPa
$\alpha_{1,2}$	702, 31
β_0, γ_0	0.039, 0.15
$\gamma_{1,2,3,4}$	0.92, −4000, 0.0063, 2.89
β	20

$$de_{11} = \frac{ds_{11}}{2\mu[1-\frac{3}{2}(s_{11}-r_{11})^2\Gamma]} \tag{16}$$

in which

$$a = \frac{1}{Cs_y^0[f(z)]^2}. \tag{17}$$

For simplification, in this work the material constants β_r and γ_r are chosen as follows (Peng and Ponter, 1993):

$$\beta_r = \beta_0\alpha_r, \quad \gamma_r = \gamma_0, \quad r = 1,2. \tag{18}$$

4. THEORETICAL CORRELATION

Using the method developed by Peng and Ponter (1993) and Watanabe (1986) the material constants and parameters involved in this model can be determined. The material constants and parameters so determined for rail steel BS11 are given in Table 4.

The analytical relation between P and ε for the segment 1 of test 2 is shown in Fig. 5(b), in which it is seen that the variation of P is satisfactorily described compared with the experimental result shown in Fig. 5(a). The theoretical hysteresis loops corresponding to the last strain cycle of each segment in test 2 are plotted in Fig. 6(b), which is in reasonable agreement with the experimental result shown in Fig. 6(a).

The analytical variation between load P and strain ε for test 6 is plotted in Fig. 10(b), which describes the main characteristics of the experimental result shown in Fig. 10(a). The theoretical variation of both ε_m and $d\varepsilon_m/dN$ during the cyclic process is shown in Figs 10(c) and (d), from which it is seen that the result given by the present model fits the cyclic ratcheting process well, and the property that the ratcheting rate tends to constant during cyclic process is also well described. The result corresponding to the segments 1 and 5 in test 7 is shown in Figs 11(a) and (b), respectively. Compared with the experimental data the theoretical results also describe reasonably the ratcheting and its rate in the cyclic process.

5. CONCLUSION

A detailed experimental investigation for mechanical behaviour of rail steel BS11 subjected to uniaxial cyclic loading has been made in this work. The following main properties have been observed:

1. There exists no distinct yield point. The transition from elastic deformation to plastic hardening is gradual and smooth.

2. Strong strain hardening is observed in monotonic loading. Compared with the constitutive response in cyclic process, it is found that the hardening is mainly kinematic.

3. Cyclic softening is observed when a cyclic loading process follows a monotonic one, but this kind of softening decreases as strain amplitude increases and vanishes when strain amplitude reaches around 1.2%. It is also observed that the saturated hardening state is only slightly affected by deformation history.

4. Negative mean stress is detected even in a symmerically strain-controlled test, which may probably be attributed to the existence of defects such as micro-cracks in the material and these defects reduce the effective area of the cross section of the specimen.

5. In a strain-controlled cyclic process, if ε_m exists, σ_m will relax to a value corresponding to the given ε_m. Generally σ_m increases when ε_m increases, provided the strain amplitude is fixed. Similarly ε_m increases when σ_m increases in stress-controlled process provided the stress amplitude is fixed.

6. σ_a mainly depends on ε_a and is slightly affected by ε_m. If ε_a is chosen constant, σ_a decreases slightly while σ_m increases. Conversely if σ_a is chosen constant, ε_a increases slightly while σ_m increases. This relation is almost independent of deformation history.

7. The steady ratcheting rate is mainly determined by σ_m and σ_a. $\mathrm{d}\varepsilon_m/\mathrm{d}N$ increases if either σ_a or $|\sigma_m|$ increases. There is no indication that ratcheting will stop in the above tests even if the specimen was subjected to thousands of cycles to fracture.

The theoretical correlation covered some experimental observation. These results show that the constitutive equation developed by Peng and Ponter (1993) and Fan and Peng (1991) is able to describe the main mechanical properties of rail steel BS11 in cyclically plastic deformation process.

Acknowledgements—The authors gratefully acknowledge the support of the British Council of Great Britain through an academic exchange agreement between the University of Leicester and Chongqing University. Thanks are also due to both universities for actively supporting this academic link.

The authors are also grateful to Mr C. J. Morrison and Dr J. Garnham for their help in many aspects of this work.

REFERENCES

Bower, A. F. (1987). The influence of strain hardening on cumulative plastic deformation caused by repeated rolling and sliding contact. University of Cambridge, CUED/C-Mech/TR. 39.

Bower, A. F. (1989). Cyclic hardening properties of hard-drawn copper and rail steel. *J. Mech. Phys. Solids* **37**(4), 455–470.

Bower, A. F. and Johnson, K. L. (1990). Plastic flow and shakedown of rail surface in repeated wheel–rail contact. *Third International Symposium Contact Mechanics and Wear of Rail–Wheel Systems*. Cambridge, U.K.

Fan, J. and Peng, X. (1991). A physically based constitutive description for non-proportional cyclic plasticity. *J. Engng Mat. Tech.* **113**, 254–262.

Peng, X. and Ponter, A. R. S. (1993). A constitutive law for a class of two-phase materials with experimental verification. *Int. J. Solids Structures*. (To be published.)

Watanabe, O. and Atluri, S. N. (1984). Constitutive modelling of cyclic plasticity and elastoplasticity with isotropic or kinematic hardening. *Comput. Mech. Appl. Mech. Engng* **43**, 134.

Watanabe, O. (1986). The determination of material constants for cyclic plasticity with a new integrating form of endochronic constitutive equation. Personal communication (in Japanese).

Wu, H. C. and Yang, R. J. (1983). Application of improved endochronic theory of plasticity to loading with multiaxial strain path. *J. Non-linear Mech.* **18**, 395–408.